Steam Reforming of Ethanol over Ni/Al2O3–La2O3 Catalysts Synthesized by Sol–Gel

ARTICLE *in* INDUSTRIAL & ENGINEERING CHEMISTRY RESEARCH · OCTOBER 2010

Impact Factor: 2.59 · DOI: 10.1021/ie100636f

6 AUTHORS, INCLUDING:

Raul Carrera-Cerritos
Instituto Politécnico Nacional
8 PUBLICATIONS **80** CITATIONS
SEE PROFILE

R. Fuentes-Ramirez
Universidad de Guanajuato
31 PUBLICATIONS **118** CITATIONS
SEE PROFILE

J. Merced Martínez-Rosales
Universidad de Guanajuato
16 PUBLICATIONS **145** CITATIONS
SEE PROFILE

Tomás Viveros-García
Metropolitan Autonomous University
67 PUBLICATIONS **536** CITATIONS
SEE PROFILE

I&EC research
Industrial & Engineering Chemistry Research

ARTICLE

pubs.acs.org/IECR

Steam Reforming of Ethanol over $Ni/Al_2O_3-La_2O_3$ Catalysts Synthesized by Sol−Gel

Raúl Carrera Cerritos,[†] Rosalba Fuentes Ramírez,[†] Alberto F. Aguilera Alvarado,[†] J. Merced Martínez Rosales,[†] Tomás Viveros García,[‡] and Ignacio R. Galindo Esquivel*[,†]

[†]División de Ciencias Naturales y Exactas, Departamento de Ingeniería Química, Universidad de Guanajuato, Noria Alta s/n, Col. Noria Alta, C. P. 36050 Guanajuato, Gto., México

[‡]División de CBI, Departamento de IPH, Universidad Autónoma Metropolitana, Rafael Atlixco No. 186, Col. Vicentina, C. P. 09340, Iztapalapa, D.F., México

ABSTRACT: The activity of $Ni/Al_2O_3-La_2O_3$ catalysts prepared by sol−gel process for hydrogen production using ethanol steam reforming was studied. The effect of Ni and La loading in the reaction activity and hydrogen selectivity was analyzed. The catalytic measurements were performed on a fixed-bed microreactor for a 6 h period; within this time, the catalysts showed partial deactivation. The catalyst containing 12 wt % La showed the highest yield to H_2, but it also presented the highest deactivation. The other catalysts with the same Ni loading showed a decrease in H_2 yield over time. The increase of Ni loading from 5 to 10 wt % caused an increase in H_2 and CO yields in all La containing catalysts. The catalyst supported on sol−gel synthesized alumina showed the highest activity after 6 h on stream. This catalyst showed the lowest deactivation from all the systems that were studied. Polymeric and graphitic carbon were identified by DTA analysis of the spent catalysts. TGA analysis showed that the total coke deposited after reaction followed the trend: Ni/Al > Ni/12La ≈ Ni/8La > Ni/5La. However, less graphitic coke was identified on the catalysts as the lantana loading increased in the supports. Additionally, TEM results indicate that the radius of the graphite tubes decreased as the concentration of La in the support increased. A slight increase of H_2 and CO_2 yields was obtained when the water to ethanol mole ratio increased from 3 to 6. Higher deactivation was observed when more steam was fed to the reaction, even when lower carbon contents were determined by DTA-TGA analysis.

1. INTRODUCTION

The world's energy production is dominated by fossil fuels as energy sources; petroleum is the most versatile of the fossil fuels with high energy density and ease of transportation. Nevertheless, the limited reserves, instability of prices, and the environmental problems caused by the use of fossil fuels has brought forward intensive research from both academia and industry to substitute the fossil fuels with alternative biorenewable clean fuels.

The automotive sector represents a special challenge as the energy conversion is strongly decentralized. So far, oil-derived products have been the solution, but a number of alternative fuels are being considered, such as LPG, natural gas, methanol, DME, ethanol, biodiesel, syn-fuels, and hydrogen.[1] The use of fuel cells for electric power generation in automobiles has immense potential since they offer high efficiency with environmental and operational benefits when compared to conventional technologies.[2] Unlike fossil fuels, hydrogen that is used as feed in fuel cells has some benefits as it burns cleanly, without emitting any environmental pollutants. In addition, hydrogen is abundantly available in the universe and possesses the highest energy content per unit of weight (i.e, 120.7 kJ/g), compared to any of the known fuels. Hydrogen is considered to be the energy carrier of the future and could have an important role in reducing environmental emissions.[3]

One possibility to obtain energy from renewable sources is related to fermentation of organic matter to produce bioethanol. It has been suggested that instead of using this ethanol in internal combustion engines, it could be used to generate hydrogen for, more efficient, fuel cell applications through the ethanol steam reforming reaction.[4] For this process to be economically feasible, it is necessary to identify catalysts that must be active and selective to hydrogen at low temperature. Additionally the catalysts should decrease coke formation to avoid their deactivation. Considering this scenario, several catalysts have been tested in steam reforming of ethanol, including those based on noble and non-noble metals.[5]

Among transition metals, Ni-based catalysts pose a good alternative for ethanol steam reforming reactions because this metal has a relatively low cost when compared to other transition metals, it has been observed to be considerably active during C−C bond scission reaction steps, and particularly, it has well-known high activity toward dehydrogenation reactions.[6] From a practical point of view and to maximize the exposed surface of Ni, the metal is normally deposited over a high surface area support such as γ-Al_2O_3, which is widely used due to its good mechanical properties and relatively low cost.[7] However, the production of ethylene is generally favored over acidic supports (such as γ-Al_2O_3). Ethylene formation is undesirable, since it has been associated to coke formation and catalyst deactivation.[8] One alternative that has been explored consists in the neutralization of

Special Issue: IMCCRE 2010

Received: March 15, 2010
Accepted: August 25, 2010
Revised: August 6, 2010
Published: October 11, 2010

dx.doi.org/10.1021/ie100636f | *Ind. Eng. Chem. Res.* 2011, 50, 2576–2584

γ-Al_2O_3 surface acidic sites through the addition of basic metal oxides, such as MgO or La_2O_3.[9]

The alumina-lanthana carrier is known to decrease deactivation and enhance the selectivity to hydrogen in comparison to the frequently used γ-alumina.[7,10,11] It is also known that La can affect (i) the hydrogen activity of the supported metals, (ii) the thermal stability of textural and structural properties of γ-Al_2O_3, and (iii) control carbon formation during methane reforming.[12] In fact, Ni/La_2O_3 catalysts exhibit high activity, stability, and selectivity toward hydrogen during steam reforming of ethanol. However, lanthanum oxide is hygroscopic and pellets prepared with this material do not possess the necessary stability and mechanical strength in the presence of high concentrations of steam, especially at low temperatures. This problem may be avoided if lanthana is dispersed over materials that exhibit the necessary strength and stability, such as alumina.[13] Furthermore, the homogeneous distribution of lanthanum crystals on the carrier may play an important role on decreasing deactivation of the catalysts. For example, it has been proposed that lanthana addition to Ni/Al_2O_3 catalysts significantly enhances the catalytic activity and stability in the steam reforming of propane because of the presence of lanthanides that avoid both the growth of nickel crystallites and the reoxidation of metallic nickel sites during the reaction.[14]

The sol−gel method is a successful way to obtain homogeneous alumina−lanthana mixed oxides with high surface area, high porosity in the mesoporous range, and good thermal stability,[15,16] In the present work, the activity on steam reforming of ethanol over Ni/Al_2O_3−La_2O_3 catalysts prepared by the sol−gel method for the production of hydrogen is investigated. The effect of Ni and La loading in the catalytic activity of the materials was analyzed. In addition, the water to ethanol mole ratio in the feed stream of the reactor was modified for the catalyst that presented the highest H_2 yield. Thermal gravimetric analysis (TGA-DTA), X-ray diffraction (XRD), and temperature programmed reduction (TPR) techniques were used to characterize the catalysts.

2. EXPERIMENTAL SECTION

2.1. Catalysts Preparation. One hundred milliliters of isopropylic alcohol (99.7%, JT Baker) was placed in a glass reactor with the appropriate amount of lanthanum nitrate hexahydrated (99%, Aldrich) corresponding to 5, 8, and 12 wt % (named 5La, 8La, and 12La, respectively). The mixture was left under stirring at 300 rpm. After 1 h, aluminum tri-sec-butoxide (97%, Aldrich) was injected into the reactor, and the system was left under stirring for 1 h. Afterward, the reactor was cooled to 277 K to perform the hydrolysis. The hydrolysis mixture, containing HNO_3 (70%, Aldrich) and distilled water, was added dropwise into the system at constant rate of 0.35 mL/min. Once the hydrolysis mixture was added, a sol was formed, which turned into a gel after a few minutes. The gel was left at ambient temperature for an aging period of 24 h. Finally, the gel was dried at 308 K and calcined at 973 K for 2 h. An alcohol/water/acid/alkoxide molar ratio of 80:30:0.2:1 was used in all synthesis.

Ni catalysts were prepared by incipient wetness impregnation of each of the above supports using aqueous solutions of $Ni(NO_3)_2 \cdot 6H_2O$ (Aldrich). Ni loading in the different catalysts was 10 and 5 wt % (named 10Ni and 5Ni, respectively). After Ni incorporation, the samples were dried at 298 K for 24 h and subsequently calcined in air at 973.15 K for 2 h.

2.2. Characterization. Surface area (S_{BET}) and pore volume (V_p) of the calcined lanthana−alumina supports and 10Ni catalysts were obtained by N_2 adsorption−desorption isotherms at 77 K using a Micromeritics ASAP 2010 instrument, and pore size distribution was determined by the Barret−Joyner−Hallenda (BJH) method applied to the desorption branch of the nitrogen isotherm.

Crystalline phases of the catalysts were identified by XRD using a Rigaku Mineflex instrument operated with monochromatic Cu−Kα radiation. The patterns were collected from 2θ = 20 to 80° with a step size of 2°/min.

The reduction properties of the catalysts were analyzed by using an ISRI RIG-100 instrument with 60 mL/min of 10% hydrogen in argon flow. The hydrogen consumption was measured by a TCD detector from ambient to 1173 at 10 K/min.

The carbon deposition was measured by TGA-DTA analysis of the used catalyst, which was carried out with a thermogravimetric balance Netzsch, STA-409EP. It was performed from ambient to 1273 K with a heating rate of 10 K/min in static air.

TEM analysis of the 10Ni catalysts after reaction tests were conducted in a Jeol JEM-100S apparatus operated at 60 kV.

2.3. Activity Test. Fifty milligrams of catalyst (particle size between 120−150 tyler mesh) were diluted with 0.6 g of quartz (mesh 80−100). This mixture was placed into a 10 mm i.d. and 30 cm length quartz reactor. The catalytic bed (7 mm high) was kept in place by means of quartz wool. The reactor temperature was measured by means of a K-type thermocouple placed over the catalytic bed. The catalysts were reduced in situ at 923 K for 2 h (heating rate 10 K/min) with a hydrogen flow of 50 mL/min. After reduction, the system was flushed with 50 mL/min of argon for 15 min. The resulting catalyst was tested in steam reforming of ethanol, as follows: A liquid flow of 1 mL/h of water−ethanol (water/ethanol (mol/mol) = 3, VHSV = 11500 $cm^3/kg_{cat} \cdot h$, based on liquid ethanol flow) was obtained by sending an independent argon flow to water and ethanol saturators; the water saturator temperature was 343 K, while ethanol saturator was 303 K. The ethanol and water streams were mixed and adjusted with pure argon until a total flow of 100 mL/min was measured. The tubing was insulated and heated to avoid condensation of the reactants. The composition of the reactor effluent was analyzed by means of two gas chromatographs: the first one (HP 5890 series II), equipped with a HP-1 capillary column, a FID detector, and Ar as carrier gas, was used for the separation of C_2H_5OH, CH_3CHO, C_2H_4, CH_3COOH, and CH_3COCH_3. The second gas chromatograph (Gow-mac series 580) equipped with a Carbosphere packed column and a TCD detector was placed on line and was used for the analysis of H_2, CO, CH_4, and CO_2.

3. RESULTS

3.1. Nitrogen Adsorption−Desorption. BET specific surface area, mean pore size diameter, and pore volume results are reported in Table 1. Pure alumina presented the highest specific surface area (300 m^2/g) and pore volume (0.79 cm^3/g). A minimal reduction in the specific surface area and pore volume was detected for the 5La support. On the other hand, a larger reduction of surface area and pore volume was observed for the 8La and 12La supports.

After nickel impregnation all the catalysts show a diminution on the surface area when compared to the original support. The surface area for the 10Ni/Al catalyst in comparison to the Al

Table 1. BET Surface Areas (S_{BET}), Pore Volume (V_p), and Average Pore Diameter (D_p) of Synthesized Supports and 10Ni Catalysts

sample	S_{BET} (m^2/g)	V_p (cm^3/g)	D_p (Å)
Al	300	0.79	111
5La	280	0.76	109
8La	232	0.61	105
12La	220	0.65	117
10Ni/Al	219	0.61	111
10Ni/5La	212	0.57	108
10Ni/8La	174	0.44	101
10Ni/12La	168	0.42	99

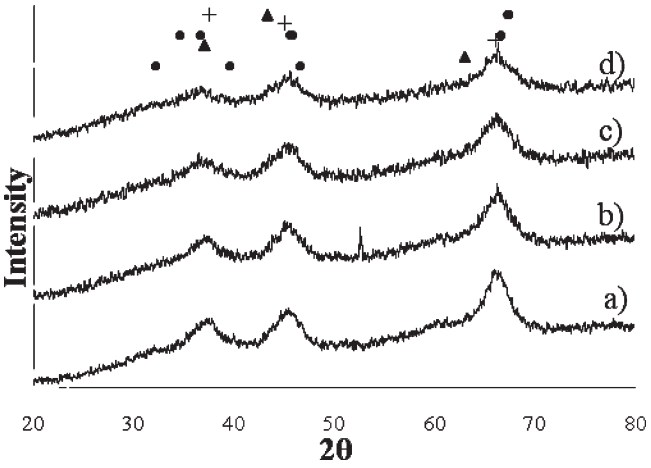

Figure 1. XRD patterns of 10 wt % Ni catalysts calcined at 973 K: (a) Al, (b) 5La, (c) 8La, and (d) 12La; (●) γ-Al_2O_3, (▲) NiO, and (+) $NiAl_2O_4$.

support decreased by −80 m^2/g, this is the highest decrease observed after impregnating all supports. The diminution in surface areas after impregnation is less pronounced as the lanthanum content increases. In all cases the pore volume decreased by approximately 0.20 cm^3/g. The average pore diameter was approximately the same after Ni impregnation for Al, 5La, and 8La supports. After impregnation of the 12La support, the average pore diameter decreased considerably. This diminution could be related to some sort of surface rearrangement, since the observed surface area decrease is the lowest from all the materials and does not point toward pore plugging. The results suggest that nickel impregnated homogeneously on all the supports.

3.2. XRD. The X-ray diffraction patterns of reduced catalysts calcined at 973 K are shown in Figure 1. The relative intensities of the peaks centered at $2\theta = 37.5, 45, 66.2°$ correspond to γ-Al_2O_3, but the position of the signals is closer to $NiAl_2O_4$ phase (2θ = 37.5, 44.8, 66.7) rather than γ-Al_2O_3 ($2\theta = 36.57, 45.58, 66.55°$). This could suggest the presence of a solid composed by a mixture of both compounds. However, it should be considered that the original supports calcined at 973K did not show any reflections, indicating a microcrystalline or amorphous nature; therefore the presence of a well developed γ-Al_2O_3 phase is considered to be less likely. In addition, a weak reflection at $2\theta = 52.48°$ corresponding to NiO is detected for the 10Ni/5La catalyst. The intensity of the observed reflections diminishes as the La loading increases; this indicates that the crystallite size of the detected species decreases with the increase in La loading. Considering

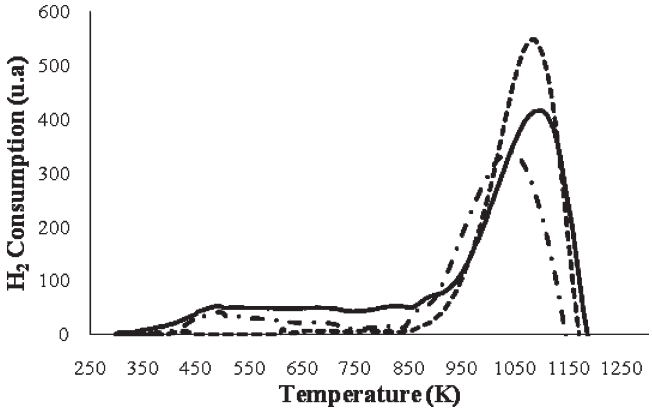

Figure 2. H_2-TPR curves of 10 wt %. Ni catalysts: (—) Al, (- · -) 5La, and (- - -) 8La.

that the identified reflections are more likely due to $NiAl_2O_4$ phase formation, the observed decrease of the samples crystallite size associated to the La loading increase, suggests that lanthanum inhibits this phase formation.

3.3. TPR. Temperature-programmed hydrogen reduction (H_2-TPR) of the Ni/Al and La containing catalysts can give information on the influence of La_2O_3 on the interactions between Ni and alumina. The TPR profiles of the Ni/Al and Ni/5La catalysts show two reduction peaks (Figure 2). The first one appearing at 350−850 K can be associated with the reduction of nickel species with weak interaction with support. The main peak centered at ∼1050 K is related to the reduction of $NiAl_2O_4$ species with the strongest interaction with support. For the Ni/8La, only the last reduction peak was observed. This agrees with the TPR for $NiO/La_2O_3/Al_2O_3$ catalysts prepared by sol−gel.[9] On the other hand, previously reported H_2-TPR studies of $Ni/La_2O_3/\alpha$-Al_2O_3 catalysts prepared by impregnation show three peaks at low temperature and a peak at high temperature (890−1033 K). The presence of the new high-temperature peak was associated with the existence of the Ni species with increased interaction with the support after the addition of La_2O_3 on the catalysts.[17] In addition, three reduction peaks (818, 942, and 1041 K) were reported for $Ni/La_2O_3/\gamma$-Al_2O_3 prepared by impregnation; the reduction peaks were attributed to reduction of NiO species with weak interaction with alumina support, to reduction of highly dispersed nonstoichiometric amorphous nickel aluminate spinels, and to a diluted $NiAl_2O_4$-like phase, respectively.[10] However, the degree of the interaction could differ because of the different preparation methods.

Hydrogen consumption profiles for Ni/*x*La catalysts are similar to that obtained for Ni/Al (Figure 2). The main reduction peak shifted toward lower temperature for samples with 5 wt % La_2O_3 content; this suggests that reduction properties of the Ni species are improved at low lanthana concentrations. On the other hand, the broad shoulder related to the reduction of Ni species with weak interaction with the support becomes smaller with the increase of La_2O_3 loading. Diminution of the bands associated to weakly interacting Ni species was also observed in $Ni/La_2O_3/\gamma$-Al_2O_3 prepared by the impregnation method, and it was associated to the presence of surface species containing Ni, Al, and La derived from a strong interaction between Ni and La ions.[10] In that work, the peak corresponding to nickel with weak interaction with the support was still detected even at 15% La

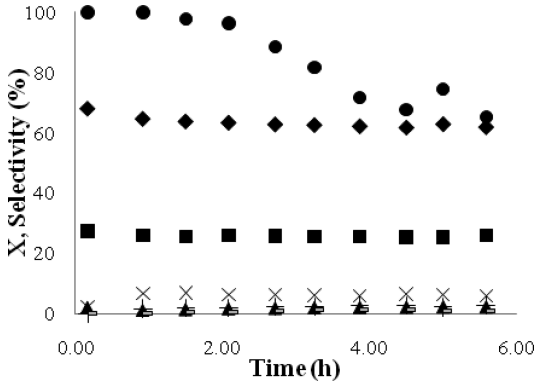

Figure 3. Ethanol conversion and product selectivity during steam reforming of ethanol over 10Ni/12La catalyst (50 mg catalyst, T = 873 K, water/ethanol (mol/mol) = 3, Total flow = 100 mL/min, ethanol flow = 1.644E^{-4} mol/min). (●) Conversion, (♦) H_2, (■) CO, (▲) CH_4, (×) CO_2, (+) C_2H_4, (−) CH_3CHO.

loading. In the present research, Ni with weak interaction was not detected even at 8% La loading (Figure 2). The sol−gel method could be responsible for the increased interaction between Ni species and the support.

3.4. Activity Test. *3.4.1. Influence of La_2O_3 Loading.* The product selectivity was defined as the mol % of each product and the product yield was calculated as the product/ethanol reacted mole ratio. The selectivity and conversion (X) over 10Ni/12La is shown in Figure 3 as a representation for what is observed in all the systems over reaction time. The figures of the other catalysts present similar trends and are not presented, only the distinctive features for each system are discussed. As it is observed 100% conversion is obtained at the beginning of the reaction. However, the catalysts began to deactivate after ∼1.5 h on stream. The decrease in activity is considerable, since after only 5.5 h on stream the conversion reaches a value of ∼70%. All 10Ni catalysts showed a similar behavior regarding ethanol conversion, which remained at 100% up to 2.0, 2.75, and 3.5 h over 10Ni/8La, 10Ni/5La, 10Ni/Al catalysts, respectively. At higher La contents, the deactivation of the catalysts took place sooner. The conversion after 5.5 h reaction time was similar in all 10Ni catalysts (65−73%). A decrease in activity as the La content increases has been reported for the ethanol steam reforming over bare Al_2O_3−La_2O_3 supports.[10] These authors also showed that the catalytic activity, of 17Ni/3La_2O_3/Al_2O_3 catalyst prepared by incipient wetness impregnation was similar to 17Ni/Al_2O_3. They observed that the catalysts with 6% La showed the highest deactivation from all the catalysts tested reaching 80% ethanol conversion in the first 20 h on stream. It is important to indicate that lower VHSV were used in the previous work, when compared to the present research. This lower VHSV justifies the increased lifespan observed on the previously reported catalysts.[10]

Initially the selectivity toward H_2, CO, CO_2, and CH_4 of 10Ni/12La was 68, 27, 2, 2 mol %, respectively. The selectivity to H_2 progressively decreased with reaction time because of catalyst deactivation. The CO, CO_2, and C2 compounds selectivity was nearly constant in all catalysts. The presence of CH_3CHO and C_2H_4 suggests that ethanol dehydrogenation (reaction 1) and dehydration (reaction 2) reactions are taking place

$$CH_3CH_2OH \rightarrow CH_3CHO + H_2 \quad (1)$$

$$CH_3CH_2OH \rightarrow C_2H_4 + H_2O \quad (2)$$

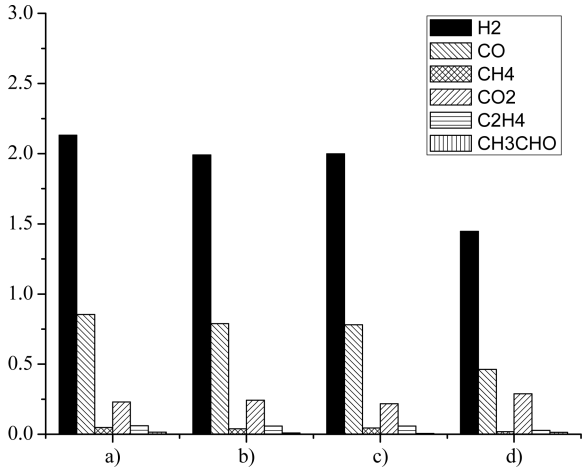

Figure 4. Reaction yields after 1.5 h on stream and 100% conversion, of Ni 10 wt. catalysts: (a) 12La, (b) 8La, (c) 5La, and (d) Al.

The selectivity during the entire reaction was higher toward CO than the selectivity to CO_2 on all catalysts. This observation coincides with previously reported temperature programmed desorption (TPD) results obtained over 20Ni/Al_2O_3 and 20Ni/10La_2O_3/Al_2O_3 impregnated catalysts, where the main desorption products were H_2 and CO at 873 K when preadsorbing 1% ethanol and 1% H_2O.[18] This suggests that ethanol reforming with insufficient steam supply (reaction 3) and ethanol decomposition (reaction 4) could be part of the reaction path favored by these catalysts, while the water-gas shift reaction (reaction 5) is not proceeding at considerable rates.

$$CH_3CH_2OH + H_2O \rightarrow 2CO + 4H_2 \quad (3)$$

$$CH_3CH_2OH \rightarrow CH_4 + CO + H_2 \quad (4)$$

$$CO + H_2O \rightarrow CO_2 + H_2 \quad (5)$$

Figure 4 shows the product yields of the catalysts after 1.5 h on stream, at this point, ∼100% conversion was calculated in all catalysts. Higher H_2 yields on La containing catalysts (2.1, 2.0, and 2.0 for 10Ni/12La, 10Ni/8La, and 10Ni/5La, respectively) were observed, when comparing with the 10Ni/Al catalyst (1.4). CO, CO_2, C_2H_4, and CH_3CHO yields were similar independently of the La content in the catalysts. The 10Ni/Al catalyst presented a higher yield to CO_2 when comparing to the La containing materials, this increase on CO_2 formation seems to be partially associated with a decrease in CO formation. This suggests that the water−gas shift (WGS) reaction was slightly favored over the10Ni/Al catalyst. C_2H_4 and CH_4 formation was higher on the La containing catalysts than on the pure alumina supported catalyst.

The product yields of the catalysts after 6 h on stream (Figure 5) show an increase of the H_2 yield for the 10Ni/12La catalyst from the 2.1 observed after 1.5 h to 2.6 after 6 h. On the other hand, the H_2 yield remained nearly constant in all the other catalysts. Although the 10Ni/12La catalysts presented the highest H_2 yield, it also presented the highest deactivation. It has been previously suggested that the C_2H_4 formed over acidic sites is the main precursor of carbon species on the catalytic surface; therefore, it is considered to be responsible of catalytic deactivation through coke deposition.[19] The smaller amount of C_2H_4 generated on the 10Ni/Al catalyst during the reaction (Figures 4 and

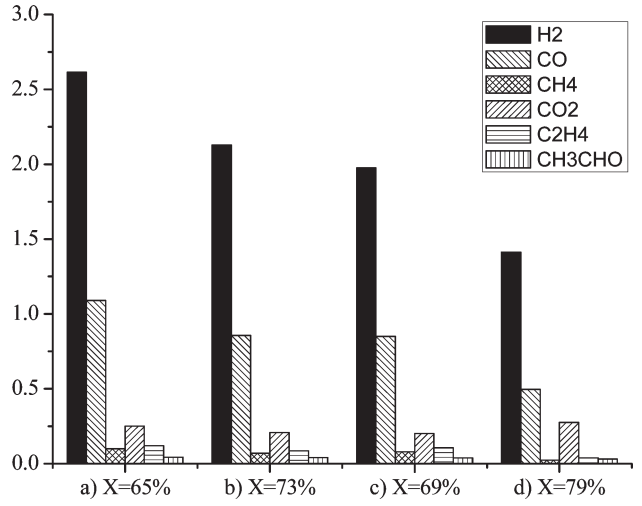

Figure 5. Reaction yields after 6 h on stream and the indicated conversion: (a) 12La, (b) 8La, (c) 5La, (d) Al.

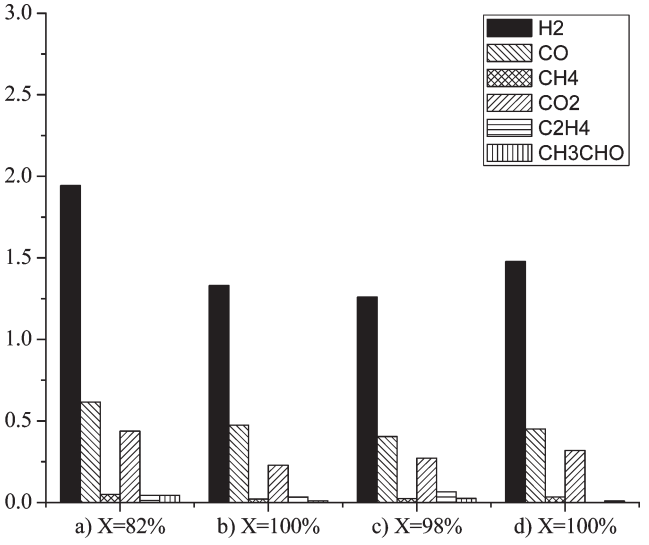

Figure 6. Reaction yields and conversion after 1.5 h on stream, of Ni 5 wt %. catalysts: (a) 12La, (b) 8La, (c) 5La, and (d) Al.

5) could explain the lowest deactivation observed in this catalysts. However, TGA-DTA studies may provide further proof regarding the source of deactivation for the La containing materials. These results are presented and discussed later.

3.4.2. Influence of Ni Loading. The effect of metal loading on the catalytic performance was studied on all the supports. Figure 6 shows the activity and product yields after 1.5 h on stream of 5 wt %. Ni catalysts. Two catalysts deactivated extremely fast, showing conversions below 100% after only 1.5 h on stream. The maximum conversion observed in these catalysts is indicated in Figure 6. When comparing Figures 4 and 6, it is possible to observe that for high nickel loadings, H_2 and CO yields are significantly higher in all La-containing catalysts. On the other hand, pure alumina-supported catalysts show approximately the same yields of all compounds independent of the Ni loading. This result agrees with those reported for Ni/Al_2O_3 when the metal is deposited by impregnation method.[20,21] The increase in H_2 and CO yields observed for high metal loadings on the La containing catalysts seems to be associated with a decrease on

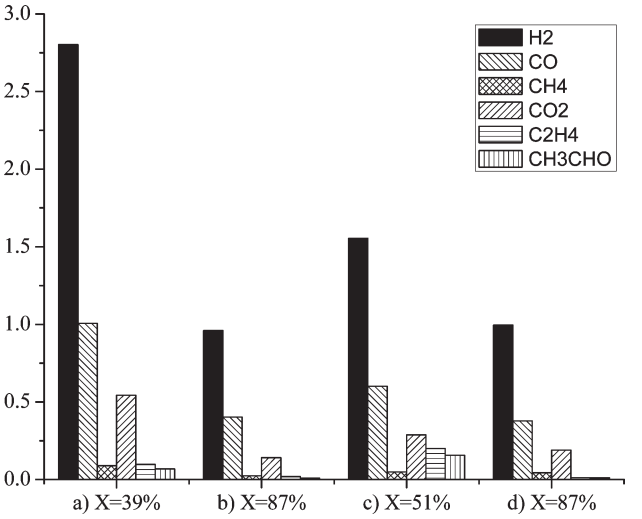

Figure 7. Product yield at 6 h on stream and the indicated conversion for 5 wt % Ni catalysts: (a) 12La, (b) 8La, (c) 5La, and (d) Al.

CH_3CHO and C_2H_4 yields. This associated decrease in C2 products for 10% Ni catalysts, suggests that Ni improves the C−C bond scission capacity of the catalyst as previously suggested by Meng Ni et al.[20] CO_2 yield decreased with the increase in metal loading for all the La containing catalysts.

Similar to what was observed in the 10Ni catalysts, the highest yield of H_2 observed on the 5Ni catalysts was detected on the catalyst supported on 12La. Pure alumina-supported 5Ni catalyst showed a slightly higher H_2 yield than 5Ni/5La and 5Ni/8La after 1.5 h on stream.

After 6 h on stream (Figure 7), the 5Ni/12La catalyst showed the highest deactivation, but kept the highest H_2 yield. The catalysts that deactivated after only 1.5 h on stream (5Ni/12La and 5La) continued to show the lowest activity after 6 h on stream. On the other hand, 5Ni supported on Al and 8La showed more stability and kept a high conversion (87%) after 6 h on stream. H_2 and CO yields were higher in almost all 10Ni catalyst at the end of the reaction, as before Ni supported on 12La was the exception, and showed higher H_2 and CO yields after 6 h with low Ni loadings.

The two 5Ni catalysts that deactivated faster (12La and 5La supported) showed a high CH_3CHO yield after 6 h on stream; this indicates that ethanol dehydrogenation (reaction 1) could be important at low ethanol conversions. This phenomenon has also been observed over Ni/CeO_2-ZrO_2.[22]

3.4.3. Influence of Water/Ethanol Mole Ratio. Thermodynamics indicate that water to ethanol feed mole ratios higher than 4 favor hydrogen yields close to 4. High water to ethanol mole ratios also avoid carbon formation. Thermodynamically a maximum of almost 5.5 H_2 yield can be obtained during ethanol steam reforming, at temperatures between 873 and 973 K and atmospheric pressure, when using steam to ethanol ratios above 6.[23] To improve the performance of the 10Ni/12La catalyst, which showed the highest H_2 yield among all the tested catalysts, an experiment using a water to ethanol mole ratio = 6, was carried out. For this experiment, the ethanol flow was kept constant and the water flow was increased, the balance with argon was such that a 100 mL/min total flow was maintained.

Surprisingly, a lower conversion was obtained when the water to ethanol mole ratio was increased. After 1.5 h on stream, a 100% conversion was obtained when a water to ethanol mole ratio of 3

was employed, while only an 89% conversion was measured when the water to ethanol mole ratio was increased to 6. Furthermore, the H_2 yield (Figure 8) did not increase when the water to ethanol mole ratio changed from 3 to 6 after 1.5 h on stream. After 1.5 h on stream, increasing the water to ethanol mole ratio only resulted in an increase on CO_2 yield, associated with a decreased CO production. This shows that the water gas shift reaction is favored by increasing the water/ethanol mole ratio.

The effect of feeding more water in the reaction showed more distinctive characteristics after 6 h on stream. At this time on stream, a high concentration of water resulted in a higher deactivation, when the water/ethanol mole ratio was 6 the conversion reached a value of only 39%, while a water/ethanol mole ratio of 3 resulted in a conversion of 65%. Nonetheless, a high concentration of water in the feed stream also caused an increment in the H_2 and CO_2 yields after 6 h on stream, as expected from the thermodynamic analysis mentioned above. Still H_2 and CO_2 production was lower when compared to Liberatori results.[12] They studied the activity and selectivity of impregnated 17Ni/12La/Al catalyst from 500 to 900 K using a 6:1, water/ethanol molar ratio. At 873 K, they achieved a 100% ethanol conversion, H_2 selectivity of ~80%, CO_2 selectivity of ~70%, and produced only CO and CH_4 as byproducts. Considering the definitions for selectivity used by Liberatori et al.; in the present study, lower H_2, CO_2, CO, and CH_4 selectivities of 63%, 16%, 20%, and 2% were obtained, respectively. These differences could be attributed not only to a higher Ni loading (17 wt %) but also to a lower VHSV (5830 $cm^3/kg_{cat}\cdot h$).

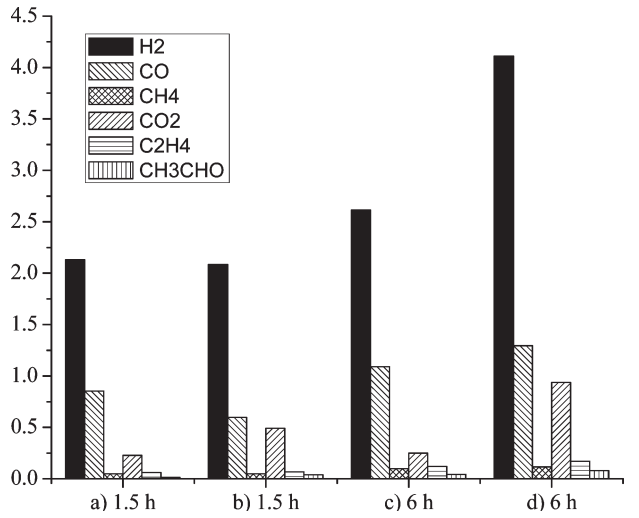

Figure 8. Reaction yields and conversion after 1.5 and 6 h on stream, of 10Ni/12La catalysts with a water/ethanol mole ratio of (a) 3 (X = 100), (b) 6 (X = 89), (c) 3 (X = 65), and (d) 6 (X = 39).

3.5. DTA-TGA Analysis of Used Catalysts. *3.5.1. Effect of Lanthana Loading.* Thermogravimetric analysis of spent catalysts after 6 h on stream is depicted in Figure 9. It was carried out to estimate the amount and type of coke deposited as revealed by weight loss because of oxidation of coke in air.

Thermograms were divided into three different temperatures intervals:[10] region I at temperatures lower than 573 K (minimal weight change) that can be ascribed to the loss of water and volatile species, such as reactants, products, and reaction intermediates. Region II at temperatures between 573 and 803 K ascribed to filamentous coke associated to Ni particles; this coke type is originated directly from ethylene polymerization reaction[18]

$$C_2H_4 \rightarrow \text{polymerization} \rightarrow \text{coke} \qquad (6)$$

Region III, located at temperatures higher than 803 K, is associated to oxidation of coke deposits with different degree of graphitization;

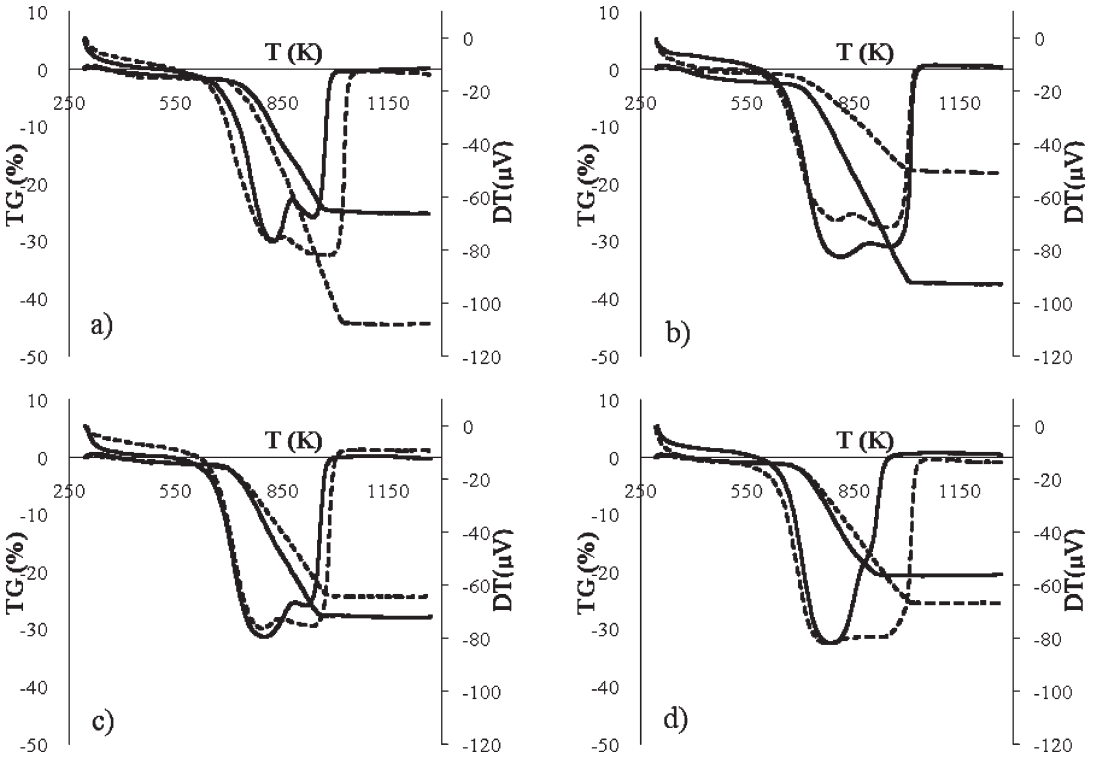

Figure 9. TGA-DTA for 5 (—)and 10%Ni (- - -) catalysts after 6 h in the steam reforming of ethanol: (a) Al, (b) 5La, (c) 8La, and (d) 12La.

dx.doi.org/10.1021/ie100636f |*Ind. Eng. Chem. Res.* 2011, 50, 2576–2584

this form of coke is attributed to dehydrogenated methyl groups (CH_x, $3 < x < 0$) formed over the carrier, in addition to carbon originating from the Boudouard reaction[18]

$$2CO \rightarrow CO_2 + C \quad (7)$$

Results show that the total coke deposited decreased in the order Ni/Al > Ni/12La ≈ Ni/8La > Ni/5La. However, the lower relative intensity in the region III indicates that coke in graphitic form decreased as the lantana loading increased.

3.5.2. Effect of Ni Loading. The amount of coke deposited over the 10% and 5% Ni spent catalysts is shown in the Figure 9. In the case of 12La catalysts (Figure 9d), a higher amount of total deposited carbon was measured when the Ni loading increased. The intensity of the signal assigned to polymeric carbon remained constant, but the signal at higher temperature increased in the 10Ni catalyst, indicating that the concentration of graphitic carbon deposited on this catalyst was higher. This type of carbon is more relevant than polymeric carbon because its accumulation results in deactivation of the catalyst.[18] Similar results were revealed in the Ni/Al catalysts (Figure 9a).

In the 5La-supported Ni catalysts (Figure 9b), a lower amount of total carbon was determined when the Ni loading increased from 5 to 10 wt %. In addition, a slight diminution of the peak intensity in region II for the 10Ni catalyst was noticed; this indicates that polymeric reactions were partially suppressed. Also, a diminution of the intensity of the peak related to graphitic carbon in 10Ni catalysts was also noted. The same phenomenon was detected on the 8La-supported Ni catalysts (Figure 9c).

Higher amounts of graphitic carbon were detected in all 10Ni catalysts, when compared to 5Ni catalysts, independently of the used support. Diminution of this type of carbon was more evident in the Al and 12La supported catalysts.

3.5.3. Effect of the Water to Ethanol Mole Ratio. The total carbon deposited after the 6 h reaction period decreases with increasing the steam content on the feed stream (Figure 10). The steam excess is believed to favor the reaction between deposited carbon and steam.[18] The intensity of the signal assigned to polymeric carbon remained identical in both steam/ethanol mole ratios studied. However, the signal at higher temperature was almost removed with the increase of steam. Diminution of solid carbon with the increased of steam was expected, but according to thermodynamic calculations, it should be absent at 873 K and water/ethanol mole ratio = 6.[24]

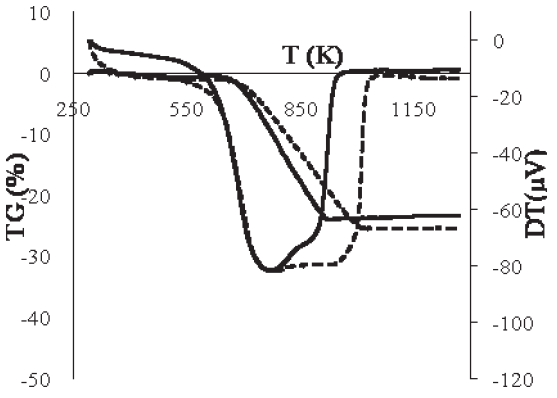

Figure 10. TGA-DTA of 10Ni/12La catalyst after 6 h under reaction with a water/ethanol mole ratio of 6 (—) and 3 (- - -).

3.6. TEM Results. The DTA-TGA analysis suggested that some graphitic carbon was formed on the catalytic surface during the reaction. To corroborate the presence of this graphitic carbon TEM micrographs of the 10Ni catalysts after reaction were taken. Graphitic carbon is expected to form long filaments that may be observed by TEM. In addition, it has been suggested that carbon filaments formed during steam reforming of propane show the same width as the Ni particle diameter where they are formed.[14,25] As it can be observed in Figure 11, there are carbon deposits in the form of long filaments in all 10Ni catalysts. The Ni/Al catalyst (Figure 11a) shows carbon filaments with two different diameters 18 and 36 nm. Considering that the carbon diameter may be related to the Ni particles diameter, the micrograph suggests that the Ni particles are in the range from 18−36 nm. XRD results of the catalyst prior to reaction suggested smaller Ni particle sizes in the catalyst, which could indicate that there was a certain degree of sintering during the reaction. The graphitic carbon observed on the 10Ni/5La catalyst (Figure 11b) presented only 18 nm diameter filaments. In the presented micrograph, there seems to be a low concentration of graphite in this catalyst surface.

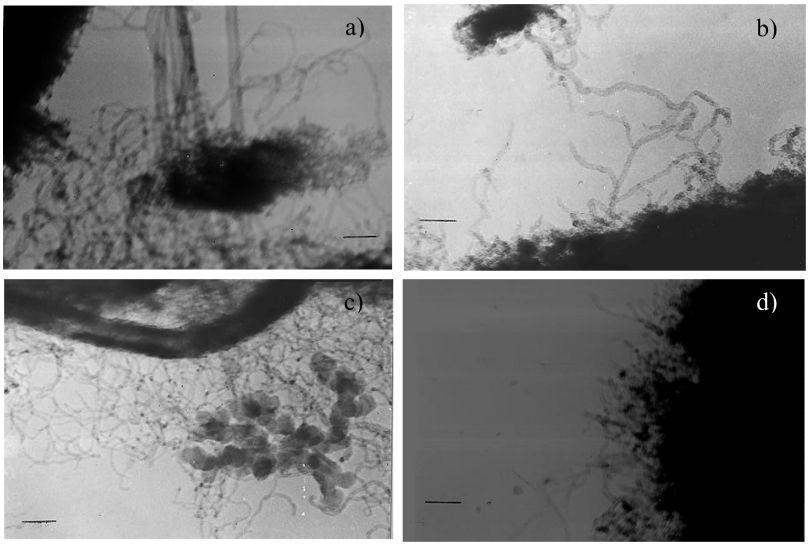

Figure 11. TEM images of 10Ni catalysts after 6 h on stream: (a) Al, (b) 5La, (c) 8La, and (d) 12La. The line length = 90 nm (100000×).

On the other hand, the amount of carbon filaments detected in the 10Ni/8La (Figure 11c) is considerable. The filaments diameter for this catalyst are of about 9 nm, this suggest higher dispersion of the Ni particles in this catalyst. Regarding the 12La-supported catalyst (Figure 11d), only a few filaments can be observed. The filaments are short and present a 9 nm diameter. The surface of this catalyst is practically free of graphitic carbon. All the above observations are in agreement with the previously presented TGA-DTA results.

4. DISCUSSION

The WGS reaction is an important step in the reforming process. During the WGS reaction, CO is converted to CO_2 and H_2 through a reversible reaction with steam. CO is an undesired product that can poison the catalyst, and therefore, the formation of CO is typically reduced by performing the reaction in excess steam.[3] It has been proposed that Ni promotes the water-gas-shift reaction,[18] still certain controversy regarding this idea remains, as other authors have found evidence the WGS reaction does not occur.[26] If the WGS reaction occurs, a CO_2/CO mole ratio close to equilibrium compositions must be expected. However, our experimental results show that CO_2/CO molar ratios do not correspond by far with the thermodynamic equilibrium predictions. Therefore, the observed results suggest that the WGS reaction is not favored on the tested catalytic systems.

Total conversion was observed in all catalysts at the beginning of the reaction. This result was expected considering that conversions higher than 90 and 99.5% were reported even at lower temperatures (320−350 °C) for the Ni/Al_2O_3 and Ni/La_2O_3 catalysts prepared by impregnation-decomposition-reduced method.[27] The deactivation of the Ni catalysts does not depend on the Ni loading and takes place sooner depending on the support, following the trend 12 La > 8 La > 5La > Al, whereas the amount of graphitic carbon decreases in the opposed order: Al > 5La > 8La > 12La. Interestingly, high carbon deposition does not correlate with high deactivation. These observations indicate that carbon deposition is not the main cause of deactivation for the studied catalysts.

The presence of lanthana is believed to improve the stability of the catalyst through the prevention of carbon deposition during the steam reforming of propane,[14] ethanol,[10] and methane.[9] It has been suggested that under reforming reaction conditions, lanthanum oxide species decorate the Ni particles and react with carbon dioxide to form $La_2O_2CO_3$ (reaction 8). Lanthanum oxycarbonate species are proposed to react with surface carbon at their periphery, thus cleaning the Ni surface from carbon deposits (reaction 9)[13]

$$La_2O_3 + CO_2 \leftrightarrow La_2O_2CO_3 \quad (8)$$

$$La_2O_2CO_3 + C \rightarrow La_2O_3 + 2CO \quad (9)$$

TGA-DTA studies after reaction show that at higher La content in the supports, the graphitic carbon present on the catalyst is minimized. This observation could provide support for the proposed La_2O_3 decoration model.

As is observed in Figure 11d, graphitic carbon was almost removed from the 5Ni/12La catalyst, this observation suggests that 5 wt % Ni is approximately the maximum loading, which can be effectively cleaned by the lanthanum species present on the 12La support under the used reaction conditions. Therefore, higher Ni loading results in an increase of metal surface, which could not be cleansed due to the insufficient lanthanum availability. This hypothesis may explain the increase of graphitic carbon detected as the Ni loading increased from 5 to 10 wt %. Furthermore, if less lanthanum is available to migrate over the metal surface when Ni content increases from 5 to 10 wt %, the diminution of Ni surface induced by La_2O_3 species migration as a source of catalytic deactivation should be minimized. Such behavior is confirmed in our results, as the 10Ni/12La catalyst deactivation is lower than that observed on the 5Ni/12La catalyst. 5Ni/12La surface is practically clean from graphitic carbon, but could be deactivated due to the Ni surface coverage by La_2O_3.

As mentioned before, the lantana containing catalysts presented higher deactivation as the lantana loading increases. TPR and XRD characterization of Ni species deposited on the carriers point toward a closer interaction between lanthanum and Ni species, which stabilizes the nickel crystallites by decreasing the crystals size upon increasing La-loading in the support. As the lanthana was highly dispersed in the support by using the sol−gel method; it could increase the close contact between Ni and La_2O_3. Therefore, it may increase the strong metal support interactions (SMSI) that promotes the partial (suboxide) or total reduction (intermetallic compounds) of La_2O_3 which could migrate over the Ni surface. This lanthana could decrease the activity of the catalysts because it lowers the accessibility of the Ni surface to the gas phase.[28] Even though an increase in La concentration on the support induced a faster and higher deactivation, the H_2 yield was also increased, which demonstrates the capability of lantana to promote hydrogen production.

The increase of the inlet steam to ethanol molar ratio from 3 to 6 caused a decrease on the graphitic carbon produced after reaction, as demonstrated by TGA-DTA. While the equilibrium of water-gas shift reaction moves forward, hence producing more CO_2 rather than CO. The increased oxidation capability created by excess water, eventually avoids carbon deposition via the Boudouard reaction. The diminution of carbon formation over the Ni/Al_2O_3 and Ni/CeO_2 catalysts in the steam reforming of ethanol by the suggested process has been previously reported.[29] However, even when the graphitic carbon diminishes when a high steam to ethanol molar ratio was used, higher deactivation is also observed. The decrease in the catalyst activity suggests that increasing the steam/ethanol ratio induces another kind of deactivation, which could be associated to an increased migration of Ni into the La_2O_3 matrix, probably hastened by the La_2O_3 hygroscopic nature.

5. CONCLUSIONS

Steam reforming of ethanol using Ni catalysts supported on Al_2O_3 and Al_2O_3−La_2O_3 prepared by the sol−gel method was studied. 100% conversion was calculated at the beginning of the reaction in all catalysts, but an early deactivation was detected in the La containing catalysts. In all catalysts, CO, CH_4, C_2H_4, and CH_3CHO byproducts were detected. The presence of C_2H_4 and CH_3CHO suggest that steam reforming is taking place by dehydration and dehydrogenation routes. On the other hand, the yields toward CO, CO_2, and H_2 suggest that WGS reaction did not occur on these catalysts at considerable rates. For 10 wt % Ni loadings, H_2 and CO yields significantly increased in all La-containing catalysts with an associated decrease on CH_3CHO and C_2H_4 yields; this associated decrease in C2 products for 10%

Ni catalysts, suggests that Ni improves the C−C bond scission capacity of the catalyst.

The catalysts deactivation takes place at earlier times depending on the support, following the trend 12La > 8La > 5La > Al; the amount of graphitic carbon decreased in the opposite order: Al > 5La > 8La > 12La. Therefore, high graphitic carbon deposition did not correlate with catalytic deactivation, which indicates that carbon deposition is not the main source of deactivation. Comparison of the catalysts with different Ni loadings shows that high Ni loadings cause an increased deposition of graphitic carbon over the catalytic surface. It is suggested that certain La species may enhance graphitic carbon elimination form the Ni surface. However, the same La species may also partially cover the Ni catalytic surface decreasing the catalysts activity and promoting the catalysts deactivation. The catalysts with 12% La presented the highest hydrogen yield when compared with the other catalysts, but they also presented the highest deactivation.

Finally, the effect of feeding more water in the reaction caused an increment on H_2 and CO_2 production after 6 h on stream, as expected. Unexpectedly, a larger deactivation is observed when more steam was fed to the reaction. The decrease in the catalyst activity does not correlate with the graphitic carbon present after reaction. The diminution of Ni surface by La species migration seems to be a more likely explanation, since the increased steam fed into the reactor may hasten the catalyst deactivation by increasing the integration of Ni into the La_2O_3 matrix, given the La_2O_3 hygroscopic nature

AUTHOR INFORMATION

Corresponding Author

*Tel.: (+52)4737320006 x1425. Fax: (+52)4737320006 x8139. E-mail: igalindo@quijote.ugto.mx.

ACKNOWLEDGMENT

We acknowledge CONACYT (México) for funding this project (No.084619), through the CB-2007 program. R.C. also thanks CONACYT for the MSc. Grant No. 213850.

REFERENCES

(1) Rostrup-Nielsen, J. R. Fuels and Energy for the Future: The Role of Catalysis. *Catal. Rev.* **2004**, *46*, 247.

(2) Cheekatamarla, P. K.; Finnerty, C. M. Reforming Catalysts for Hydrogen Generation in Fuel Cell Applications. *J. Power Sources* **2006**, *160*, 490.

(3) Haryanto, A.; Fernando, S.; Murali, N.; Adhikari, S. Current Status of Hydrogen Production Techniques by Steam Reforming of Ethanol: A Review. *Energy Fuels* **2005**, *19*, 2098.

(4) Silveira, J. L.; Braga, L. B.; Caetano de Souza, A. C.; Antunes, J. S.; Zanzi, R. The Benefits of Ethanol Use for Hydrogen Production in Urban Transportation. *Renewable Sustainable Energy Rev.* **2009**, *13*, 2525.

(5) Xuan, J.; Leung, M. K. H.; Leung, D. Y. C.; Ni, M. A Review of Biomass-Derived Fuel Processors for Fuel Cell Systems. *Renewable Sustainable Energy Rev.* **2009**, *13*, 1301.

(6) Zhang, L.; Liu, J.; Li, W.; Guo, C.; Zhang, J. Ethanol Steam Reforming over Ni-Cu/Al_2O_3-M_yO_z (M = Si, La, Mg, and Zn) Catalysts. *J. Nat. Gas Chem.* **2009**, *18*, 55.

(7) Sánchez Sánchez, M. C.; Navarro, R. M.; Fierro, J. G. L. Ethanol steam reforming over Ni/M_xO_y-Al_2O_3 (M = Ce, La, Zr and Mg) catalysts: influence of support on the hydrogen production. *Int. J. Hydrogen Energy* **2007**, *32*, 1462.

(8) Liguras, D. K.; Kondarides, D. I.; Verykios, X. E. Production of Hydrgen for Fuel Cells by Steam Reforming of Ethanol over Supported Noble Metal Catalysts. *Appl. Catal. B: Environ.* **2003**, *43*, 345.

(9) Xu, Z.; Li, Y.; Zhang, J.; Chang, L.; Zhou, R.; Duan, Z. Ultrafine NiO−La_2O_3−Al_2O_3 Aerogel: A Promising Catalyst for CH_4/CO_2 Reforming. *Appl. Catal., A* **2001**, *213*, 65.

(10) Sánchez Sánchez, M. C.; Navarro, R. M.; Fierro, J. L. G. Ethanol Steam Reforming over Ni/La−Al_2O_3 Catalysts: Influence of Lanthanum Loading. *Catal. Today* **2007**, *129*, 336.

(11) Fatsikostas, A. N.; Kondarides, D. I.; Verykios, X. E. Steam Reforming of Biomass-Derived Ethanol for the Production of Hydrogen for Fuel Cell Applications. *Chem. Commun.* **2001**, 851.

(12) Liberatori, J. W. C.; Ribeiro, R. U.; Zanchet, D.; Noronha, F. B.; Bueno, J. M. C. Steam Reforming of Ethanol on Supported Nickel Catalysts. *Appl. Catal., A* **2007**, *327*, 197.

(13) Fatsikostas, A. N.; Kondarides, D. I.; Verykios, X. E. Production of Hydrogen for Fuel Cells by Reformation of Biomass-Derived Ethanol. *Catal. Today* **2002**, *75*, 145.

(14) Natesakhawat, S.; Watson, R. B.; Wang, X.; Ozkan, U. S. Deactivation Characteristics of Lanthanide-Promoted Sol−Gel Ni/Al_2O_3 Catalysts in Propane Steam Reforming. *J. Catal.* **2005**, *234*, 496.

(15) Araujo, J. C. S.; Zanchet, D.; Rinaldi, R.; Schuchardt, U.; Hori, C. E.; Fierro, J. L. G.; Bueno, J. M. C. The Effects of La_2O_3 on the Structural Properties of La_2O_3−Al_2O_3 Prepared by the Sol−Gel Method and on the Catalytic Performance of Pt/La_2O_3−Al_2O_3 towards Steam Reforming and Partial Oxidation of Methane. *Appl. Catal., B* **2008**, *84*, 552.

(16) Barrera, A.; Viniegra, M.; Lara, V. H.; Bosch, P. Radial Distribution Function Studies of Al_2O_3−La_2O_3 Binary Oxides Prepared by Sol−Gel. *Catal. Commun.* **2004**, *5*, 569.

(17) Cui, Y.; Zhang, H.; Xu, H.; Li, W. The CO_2 Reforming of CH_4 over Ni/La_2O_3/α-Al_2O_3 Catalysts: The Effect of La_2O_3 Contents on the Kinetic Performance. *Appl. Catal., A* **2007**, *331*, 60.

(18) Fatsikostas, A. N.; Verykios, X. E. Reaction Network of Steam Reforming of Ethanol over Ni-Based Catalysts. *J. Catal.* **2004**, *225*, 439.

(19) Liberatori, J. W. C.; Ribeiro, R. U.; Zanchet, D.; Noronha, F. B.; Bueno, J. M. C. Steam Reforming of Ethanol on Supported Nickel Catalysts. *Appl. Catal., A* **2007**, *327*, 197.

(20) Ni, M.; Leung, D. Y. C.; Leung, M. K. H. A Review on Reforming Bio-ethanol for Hydrogen Production. *Int. J. Hydrogen Energy* **2007**, *32*, 3238.

(21) Alberton, A. L.; Souza, M. M. V. M.; Schmal, M. Carbon Formation and Its Influence on Ethanol Steam Reforming over Ni/Al_2O_3 Catalysts. *Catal. Today* **2007**, *123*, 257.

(22) Biswas, P.; Kunzru, D. Steam Reforming of Ethanol for Production of Hydrogen over Ni/CeO_2−ZrO_2 Catalyst: Effect of Support and Metal Loading. *Int. J. Hydrogen Energy* **2007**, *32*, 969.

(23) Rabenstein, G.; Hacker, V. Hydrogen for Fuel Cells from Ethanol by Steam-Reforming, Partial-Oxidation and Combined Auto-Thermal Reforming: A Thermodynamic Analysis. *J. Power Sources* **2008**, *185*, 1293.

(24) Rossi, C. C. R. S.; Alonso, C. G.; Antunes, O. A. C.; Guirardello, R.; Cardozo, L. Thermodynamic Analysis of Steam Reforming of Ethanol and Glycerine for Hydrogen Production. *Int. J. Hydrogen Energy* **2009**, *34*, 323.

(25) Zhang, L.; Wang, X.; Tan, B.; Ozkan, U. S. Effect of Preparation Method on Structural Characteristics and Propane Steam Reforming Performance of Ni-Al_2O_3 Catalysts. *J. Mol. Catal A: Chem.* **2009**, *297*, 26.

(26) Comas, J.; Mariño, F.; Laborde, M.; Amadeo, N. Bio-ethanol Steam Reforming on Ni/Al_2O_3 Catalyst. *Chem. Eng. J.* **2004**, *98*, 61.

(27) Sun, J.; Qiu, X. P.; Wu, F.; Zhu, W. T. H_2 from Steam Reforming of Ethanol at Low Temperature over Ni/Y_2O_3, Ni/La_2O_3 and Ni/ Al_2O_3 Catalysts for Fuel-Cell Application. *Int. J. Hydrogen Energy* **2005**, *30*, 437.

(28) Hayek, K.; Kramer, R.; Paál, Z. Metal-Support Boundary Sites in Catalysis. *Appl. Catal., A* **1997**, *162*, 1.

(29) Laosiripojana, N.; Assabumrungrat, S.; Charojrochkul, S. Steam Reforming of Ethanol with Co-fed Oxygen and Hydrogen over Ni on High Surface Area Ceria Support. *Appl. Catal., A* **2007**, *327*, 180.